

# Reduced order model of parametric resonance of electrostatically actuated MEMS cantilever resonators



Dumitru I. Caruntu\*, Israel Martinez

University of Texas-Pan American<sup>1</sup>, Mechanical Engineering Department, Edinburg, TX 78539, USA

## ARTICLE INFO

### Article history:

Received 15 October 2013

Received in revised form

25 February 2014

Accepted 25 February 2014

Available online 12 March 2014

### Keywords:

Parametric resonance

MEMS cantilever resonators

Reduced order model

Soft AC electrostatic actuation

Fringe effect

## ABSTRACT

This paper deals with parametric resonance of microelectromechanical (MEMS) cantilever resonators under soft damping, and soft alternating current (AC) electrostatic actuation to include fringing effect. A comparison between the Reduced Order Model (ROM) method and the Method of Multiple Scales (MMS) for both small and large amplitudes is reported. The actuation is parametric non-linear. It includes non-linear terms with periodic coefficients. The AC frequency is near resonator's natural frequency. The amplitude frequency response is investigated using ROM. Damping, voltage, and fringe effects on the response are also reported. It is shown that five terms ROM accurately predicts the behavior of the resonator at all amplitudes, while MMS is accurate only for small amplitudes.

© 2014 Elsevier Ltd. All rights reserved.

## 1. Introduction

Microelectromechanical systems (MEMS) gathered much attention in the past decades. Used as sensors and actuators, they are small in size, light weight, low in energy consumption and highly durable [1], and can be produced at a low cost, which makes their commercialization attractive. They can be utilized as switches, signal routing, filters, and sensors with various applications [2–5]. MEMS are inherently nonlinear. Nonlinearities usually arise from electrostatic actuation, large deformations in the structure, and squeeze film damping [6,7]. Electrostatic actuation is a frequent method used to drive miniaturized devices. This is due to its simplicity and low energy consumption [8,9]. A microbeam is deflected by direct current (DC) electrostatic load, and driven to vibrate by alternating current (AC) harmonic load [10]. Electrostatically actuated microbeam model consists of an elastic beam suspended over a ground plate. Both are made of conductive materials and a dielectric medium fills the gap between them (air gap) [11]. As the input voltage reaches a critical value, the elastic beam spontaneously deflects and collapses onto the ground plate. This behavior is known as pull-in instability and it is an important phenomenon considered in MEMS design [12,13].

Several groups investigated the dynamic behavior of MEMS. The behavior of arch resonators actuated electrically, modeled as clamped–clamped arches suspended over a ground plate, has been reported in the literature [14,15]. In Ref. [16] the non-linear response of cantilever beams to combination and subcombination resonances has been investigated using the Method of Multiple Scales (MMS). It has been found that as the frequency is swept up, the trivial solution exhibits a sudden jump as the system undergoes a subcritical pitchfork bifurcation. The beams have been assumed to have large length-to-width aspect ratios and thin rectangular cross-sections. A nonlinear clamped–clamped model of an electrostatically resonator that uses a perturbation method to predict a microbeam response to primary, superharmonic and subharmonic excitations has been reported [17]. Yet, the fringe effect has not been included. However, none of the papers mentioned reported a thorough comparison between results obtained via perturbation methods and numerical techniques for MEMS cantilever resonators to include fringe effect and soft Alternating Current (AC) actuation. The only papers reported in the literature in this respect are Refs. [18–20]. Yet, they investigated primary resonance.

This paper reports, to the best of our knowledge for the first time, a comparison between Reduced Order Model (ROM) method and the Method of Multiple Scales (MMS) for parametric resonance of MEMS cantilever resonators under soft AC actuation including fringe effect. The model of the resonator is developed using Euler–Bernoulli hypothesis. The non-linearities in the system arise from both electrostatic force and fringe effect. ROM, which is based on the Galerkin procedure, is used to develop a system of non-explicit ordinary differential equations. AUTO 07P software package for

\* Corresponding author. Tel.: +1 956 665 2079; fax: +1 956 665 3527.

E-mail addresses: [caruntud@utpa.edu](mailto:caruntud@utpa.edu), [caruntud2@asme.org](mailto:caruntud2@asme.org), [dcaruntu@yahoo.com](mailto:dcaruntu@yahoo.com) (D.I. Caruntu).

<sup>1</sup> Starting Fall 2015 University of Texas Pan American becomes University of Texas RG (Rio Grande Valley).

continuation and bifurcation problems is then used to numerically solve the system of equations, and obtain the amplitude–frequency response of the resonator. The influences of non-linearities resulting from parametric electrostatic excitation on the frequency amplitude response are reported.

## 2. Differential equation of motion

The dimensionless boundary value problem of electrostatically actuated MEMS resonators, Fig. 1, is as follows [18–20]:

$$\begin{cases} A^*(z) \frac{\partial^2 u(\tau, z)}{\partial \tau^2} + \frac{\partial^2}{\partial z^2} \left( I^*(z) \frac{\partial^2 u(\tau, z)}{\partial z^2} \right) = -b^* \frac{\partial u(\tau, z)}{\partial \tau} + \frac{\delta V^2(\tau)}{[1-u(\tau, z)]^2} + \frac{f \delta V^2(\tau)}{[1-u(\tau, z)]} \\ u(\tau, 0) = \frac{\partial u}{\partial z}(\tau, 0) = \frac{\partial^2 u}{\partial z^2}(\tau, 1) = \frac{\partial^3 u}{\partial z^3}(\tau, 1) = 0 \end{cases} \quad (1)$$

where  $z$ ,  $\tau$ , and  $u = u(z, \tau)$  are the dimensionless longitudinal coordinate, dimensionless time, and dimensionless beam deflection, respectively, and they are given by the following equations:

$$z = x/\ell; \quad \tau = \frac{1}{\ell^2} \sqrt{\frac{EI_0}{\rho A_0}} t; \quad u = w/g \quad (2)$$

In Eqs. (2)  $x$ ,  $t$ , and  $w = w(x, t)$  are the dimensional longitudinal coordinate, dimensional time, and dimensional beam deflection, respectively. Geometrical, inertial, and material properties in Eq. (2) are given by beam length  $\ell$ , gap  $g$ , reference cross-section area and moment of inertia  $A_0$  and  $I_0$ , respectively (if uniform resonator), Young's modulus  $E$ , and density  $\rho$ . For nonuniform cantilevers the reference cross-section could be where the cross-section area is maximum [21–24]. The dimensionless cross section area  $A^*$  and moment of inertia  $I^*$ , Eq. (1), are given by  $A^* = A/A_0$ ,  $I^* = I/I_0$ , where  $A$  and  $I$  are the corresponding dimensional quantities. The forces per unit length, which are at the right hand side of Eq. (1) are first damping, second electrostatic, and third fringe effect. The dimensionless parameters at the right hand side of Eq. (1) are given by the following equations:

$$b^* = \frac{b}{g} \sqrt{\frac{\ell^4}{\rho A_0 EI_0}}, \quad \delta = \frac{\varepsilon_0 W \ell^4}{2g^3 EI_0} V_0^2, \quad f = \frac{0.65g}{W}, \quad \Omega^* = \Omega \ell^2 \sqrt{\frac{\rho A_0}{EI_0}} \quad (3)$$

where  $b^*$  is the dimensionless damping coefficient,  $\delta$  is the dimensionless voltage coefficient,  $f$  is the dimensionless fringe coefficient for electrostatic force correction,  $\Omega^*$  the dimensionless frequency of excitation,  $V_0$  is the reference voltage (amplitude),  $W$  is the beam width,  $b$  is the coefficient of viscous damping per unit length, and  $\varepsilon_0 = 8.854 \times 10^{-12} \text{ C}^2 \text{ N}^{-1} \text{ m}^{-2}$  permittivity of free space. It is assumed that the resonator will operate in a viscous

pressure regime [20], therefore viscous damping force is used in this investigation. The applied voltage is given by  $V(t) = V_0 V(\tau)$  where  $V(\tau)$  is the dimensionless voltage.

## 3. Parametric resonance of uniform MEMS cantilevers

In the case of uniform cantilever resonators the dimensionless cross section area  $A^*$  and moment of inertia  $I^*$  from Eq. (1) are both equal to 1, Refs. [18–20]. Therefore, the boundary value problem of the electrostatically actuated uniform MEMS resonators is given by the following equation:

$$\begin{cases} \frac{\partial^2 u(\tau, z)}{\partial \tau^2} + \frac{\partial^4 u(\tau, z)}{\partial z^4} + b^* \frac{\partial u(\tau, z)}{\partial \tau} = \left\{ \frac{\delta}{[1-u(\tau, z)]^2} + \frac{f \delta}{[1-u(\tau, z)]} \right\} V^2(\tau) \\ u(\tau, 0) = \frac{\partial u}{\partial z}(\tau, 0) = \frac{\partial^2 u}{\partial z^2}(\tau, 1) = \frac{\partial^3 u}{\partial z^3}(\tau, 1) = 0 \end{cases} \quad (4)$$

This investigation considers soft AC actuation, small damping, and small fringe effect, i.e. parameters  $\delta$ ,  $b^*$ ,  $f$  are small. Soft AC is the voltage that produces soft electrostatic forces in the system, i.e. it produces small to very small amplitudes with respect to the gap for the MEMS cantilever resonator when the frequency of excitation is away from resonance zones. The dimensionless voltage is given by

$$V(\tau) = \cos \Omega^* \tau \quad (5)$$

The AC frequency  $\Omega^*$  is near natural frequency  $\Omega^* \approx \omega_k$ , which is written as follows:

$$\Omega^* = \omega_k + \sigma \quad (6)$$

where  $\sigma$  is a detuning parameter and  $\omega_k$  is the natural frequency. One can notice that the dimensionless electrostatic force to include the fringe effect, at the right hand side of Eq. (4), is proportional to the square of the voltage, therefore proportional to the square of the cosine function of Eq. (5). Since  $\cos^2 \Omega^* \tau = (\cos 2\Omega^* \tau + 1)/2$ , the frequency of the excitation force is a number of times greater than the natural frequency, therefore the resulting resonance is subharmonic. Moreover, since the frequency of the excitation force  $2\Omega^*$  is nearly twice the natural frequency  $\omega_k$ , the subharmonic resonance is parametric resonance. The Method of Multiple Scales (MMS) has been used to investigate the frequency response of the structure [25]. In what follows, ROM is used to investigate the dynamics of the MEMS cantilever resonators. A comparison between the two methods, namely ROM and MMS, is reported.

## 4. Reduced order model

A system of non-explicit ordinary differential equations is developed to model the frequency response of the parametric resonance of electrostatically actuated uniform MEMS cantilever resonators using ROM. This method, based on the Galerkin procedure, uses the undamped linear mode shapes of the cantilever beam as the basis functions [18–20]. The solution is assumed as follows:

$$u(z, \tau) = \sum_{k=1}^N u_k(\tau) \phi_k(z) \quad (7)$$

where  $N$  is the number of terms,  $u_k(\tau)$  are the time dependent coefficients,  $\omega_k$  are the natural frequencies, and  $\phi_k(z)$  are the corresponding set of linear undamped mode shapes of the uniform cantilever beam given by the following equation [18–20]:

$$\phi_k(z) = -\{ \cos(\sqrt{\omega_k} z) - \cosh(\sqrt{\omega_k} z) + C_k [ \sin(\sqrt{\omega_k} z) - \sinh(\sqrt{\omega_k} z) ] \} \quad (8)$$

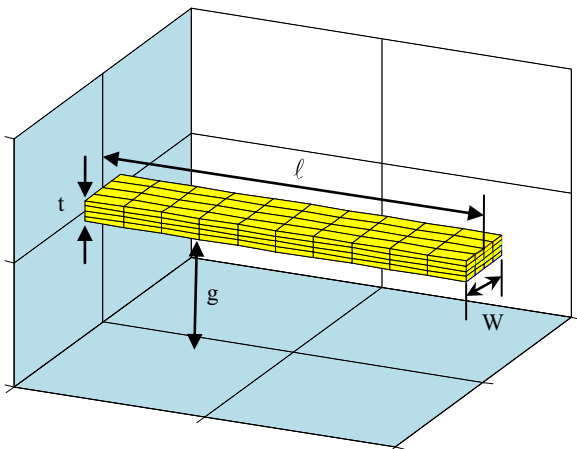


Fig. 1. Uniform MEMS cantilever resonator.

**Table 1**  
First five natural frequencies and mode shape coefficients for uniform cantilever.

	$k=1$	$k=2$	$k=3$	$k=4$	$k=5$
$\omega_k$	3.51562	22.0336	61.70102	120.91202	199.85929
$C_k$	-0.734	-1.0185	-0.9992	-1.00003	-1.00000

satisfying

$$u^{(4)} = \sum_{k=1}^N u_k \phi_k^{(4)} = \sum_{k=1}^N \omega_k^2 u_k \phi_k \quad (9)$$

and the orthonormality condition

$$\int_0^1 \phi_k \phi_p dz = \delta_{kp} = \begin{cases} 0, & k \neq p \\ 1, & k = p \end{cases} \quad (10)$$

The first five natural frequencies  $\omega_k$  and coefficients  $C_k$  from Eq. (8) are given in Table 1. In order to implement the ROM method the following steps are considered. Eq. (4) is multiplied by  $[1 - u(\tau, z)]^2$  (to eliminate any displacement  $u(z, \tau)$  from appearing in the denominator [18–20]). Eq. (7) is then substituted into it, and the resulting equation is multiplied by mode shape  $\phi_n(z)$  and integrated from  $z=0$  to 1,  $n = 1, 2, \dots, N$ . This leads to a system of  $N$  second order coupled differential equations in time as follows

$$\begin{aligned} \ddot{u}_n - 2 \sum_{ij} \ddot{u}_i u_j \int_0^1 \phi_i \phi_j \phi_n dz + \sum_{ijk} \ddot{u}_i u_j u_k \int_0^1 \phi_i \phi_j \phi_k \phi_n dz + b^* \dot{u}_n \\ - 2b^* \sum_{ij} \dot{u}_i u_j \int_0^1 \phi_i \phi_j \phi_n dz + b^* \sum_{ijk} \dot{u}_i u_j u_k \int_0^1 \phi_i \phi_j \phi_k \phi_n dz + \omega_n^2 u_n \\ - 2 \sum_{ij} \omega_i^2 u_i u_j \int_0^1 \phi_i \phi_j \phi_n dz + \sum_{ijk} \omega_i^2 u_i u_j u_k \int_0^1 \phi_i \phi_j \phi_k \phi_n dz \\ = (1+f)\delta V^2(\tau) \int_0^1 \phi_n dz - f \delta V^2(\tau) u_n \end{aligned} \quad (11)$$

where  $n=1, 2, \dots, N$ .

## 5. Numerical simulations

The system of  $N$  second order differential Eqs. (11) is transformed into a system of  $2N$  first order differential equations which is then integrated for four cases  $N=2, N=3, N=4$ , and  $N=5$  using AUTO 07P, a software package for continuation and bifurcation problems [26], which provides both stable and unstable steady-state solutions. In AUTO the computation of periodic solutions to a periodically forced system are done by adding a nonlinear oscillator with the desired periodic forcing as one of the solution components [26]. The frequency–amplitude response of the system near natural frequency is investigated using from two to five terms ROM. Table 2 gives the dimensions and the properties of the MEMS cantilever resonator used for numerical simulations. Table 3 gives the dimensionless parameters, Eq. (3), calculated with the data from Table 2.

Fig. 2 shows the parametric resonance frequency amplitude response of the MEMS resonator sensor using ROM, and a direct comparison with the method of multiple scales [25]. Solid and dash lines represent stable and unstable steady-state solutions, respectively. For both five term (5T) ROM and MMS the frequency–amplitude response consists of two nonzero steady state branches, namely branch 1, and branch 2, and zero steady state solutions branch showed as horizontal line along  $\sigma$ -axis. The response consists of two Hopf bifurcations, subcritical with the bifurcation point at A, and supercritical with the bifurcation point at B. For five terms ROM, the unstable branch 2 of the subcritical bifurcation divides the area into two distinct regions. For initial amplitudes

**Table 2**  
Dimensional system parameters.

Beam width	$W$	20 $\mu\text{m}$
Beam length	$\ell$	300 $\mu\text{m}$
Beam thickness	$h$	2.0 $\mu\text{m}$
Initial gap distance	$g$	8.0 $\mu\text{m}$
Material density	$\rho$	2330 $\text{kg/m}^3$
Young's modulus	$E$	169 GPa
Quality factor	$Q$	350
Peak AC voltage	$V_0$	12.5 V

**Table 3**  
Dimensionless system parameters.

Damping coefficient	$b^*$	0.01
Amplitude of excitation	$\delta$	0.10
Fringe correction	$f$	0.26

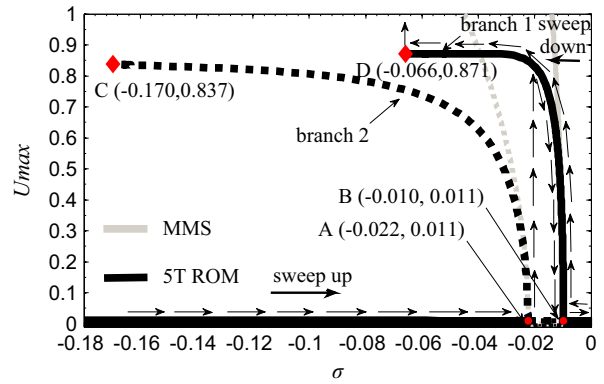


**Fig. 2.** Amplitude–frequency response, parametric resonance, using five terms (5T) ROM (present work) and MMS [25],  $b^*=0.01$ ,  $\delta=0.1$  and  $f=0.26$ .

below the dash line the system settles to zero amplitudes, while for initial amplitudes above the dash line the resonator is pulled-in (makes contact with the ground plate) or settles to large amplitudes. For a frequency less than the frequency of point C, the MEMS resonator settles to zero amplitude for any initial amplitude. When the frequency is swept up, the amplitude remains zero along the zero branch until reaches the bifurcation point A. At this point a sudden jump to higher amplitude, about 0.8 of the gap in Fig. 2, occurs. As the frequency continues to be swept up, the amplitude decreases along branch 1 until reaches bifurcation point B of zero amplitude, and continues to remain zero. When the frequency is swept down, the amplitude is zero until it reaches bifurcation point B. At this point the amplitude increases continuously until reaches point D when the MEMS resonator is pulled-in (contact of the MEMS cantilever with the ground plate, which corresponds to a dimensionless amplitude of 1, i.e. dimensional amplitude equals the gap). One can notice that for amplitudes less than 0.5 of the gap, the ROM and MMS [25] are in perfect agreement. For amplitudes larger than 0.5 of the gap MMS [25] fails to predict the behavior of the system. It underestimates the softening effect (bending to the left of the nonzero branches), and does not predict the pull-in phenomenon from large amplitudes, point D. More importantly, MMS [25] fails to predict branch 2 which shows a significant region for initial amplitudes above it from where MEMS resonators undergo a pull-in phenomenon or settle to high amplitudes.

## 6. Discussion and conclusions

MEMS cantilever resonators in this research are modeled as Euler–Bernoulli beams. No non-linearities arise from the structure

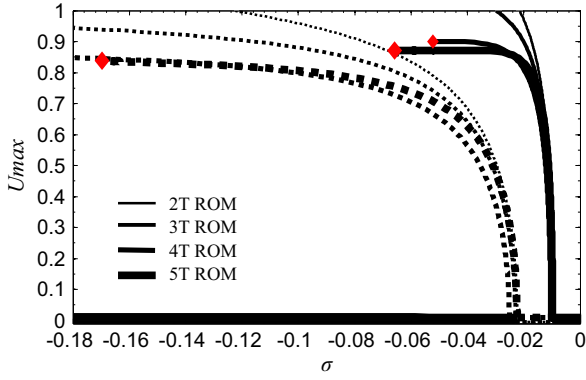


**Fig. 3.** ROM convergence for amplitude–frequency response using two, three, four and five terms ROM,  $b^*=0.01$ ,  $\delta=0.1$  and  $f=0.26$ .

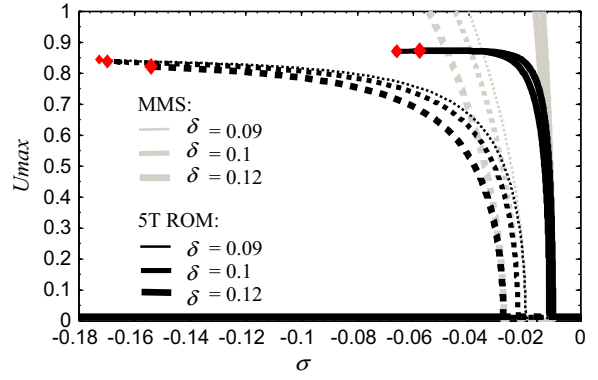


**Fig. 5.** Voltage  $\delta$  influence on the amplitude–frequency response using five terms (5T) ROM (present work) and MMS [25],  $b^*=0.01$  and  $f=0.26$ .

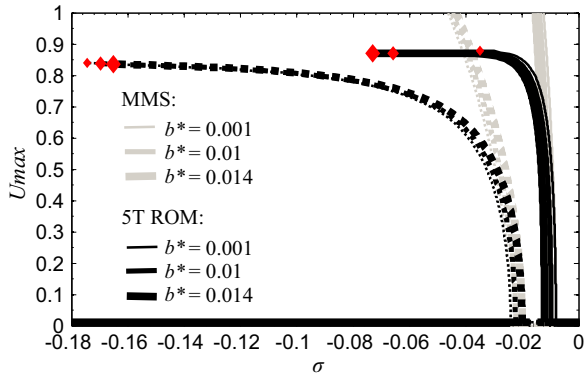


**Fig. 4.** Damping  $b^*$  influence on the amplitude–frequency response using five terms (5T) ROM (present work) and MMS [25],  $\delta=0.1$  and  $f=0.26$ .

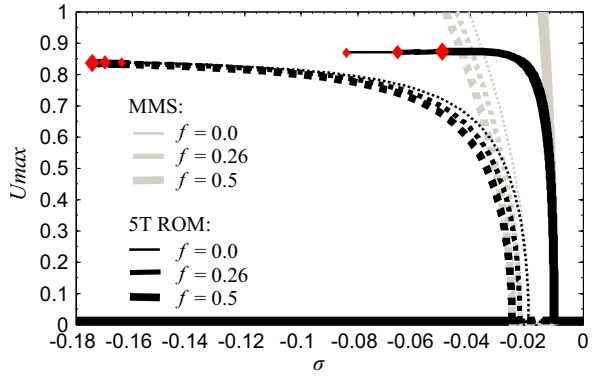


**Fig. 6.** Fringe effect  $f$  influence on amplitude–frequency using five terms (5T) ROM (present work) and MMS [25],  $b^*=0.01$  and  $\delta=0.1$ .

itself. The electrostatic force, including first-order fringe correction, actuating the resonator induces parametric nonlinear resonances. Parametric coefficients are found in both linear and nonlinear terms within the governing equation.

The ROM method in AUTO 07P is used to investigate the behavior of the system. ROM is able to accurately capture the behavior of the system where MMS [25] cannot [17], namely for moderately and large deflections up to the pull-in instability limit. Using three or more modes guarantees the convergence of the steady state amplitude [18–20]. In this work, for the frequency amplitude response of parametric resonance, it is also reported: (1) ROM convergence, Fig. 3, (2) influence of dimensionless damping, Fig. 4, (3) influence of dimensionless voltage parameter, Fig. 5, and (4) influence of the dimensionless fringe parameter, Fig. 6.

Fig. 3 shows the convergence of the ROM method in the case of frequency–amplitude response. The convergence is showed by increasing the number of terms from  $N=2$  to  $N=5$  in the ROM. As can be noted, the change becomes less significant with the addition of terms. Numerical simulations conducted in this research demonstrate that four or more terms are required for the ROM to predict pull-in, and that the five-term ROM predicts more accurately the pull-in phenomenon. One can notice that as the number of ROM terms increases, the softening effect of the MEMS resonator is better captured and points C and D better predicted. The softening effect consists of frequency decrease as the amplitude of oscillation increases.

Fig. 4 illustrates the effect of the dimensionless damping parameter  $b^*$  on the frequency–amplitude response of the resonator using a five term ROM (present work) and MMS [25]. As the damping increases the bifurcation point B and the pull-in instability point D are shifted to lower frequencies. The shifting of point D

is much more significant. Conversely, bifurcation point A and point C are shifted to higher frequencies. One can notice that increasing the damping reduces the range of frequencies for which the resonator potentially undergoes large amplitudes or pull-in phenomenon (the range of frequencies between point C and B reduces). Also the range of frequencies for which the resonator undergoes nonzero amplitudes regardless the initial amplitude reduces (the range between bifurcation points A and B). Interestingly, with the increase in damping the range of frequencies for which the resonator settles to nonzero amplitudes increases (range between points B and D).

Fig. 5 shows the influence of the voltage parameter  $\delta$  on the amplitude frequency–amplitude response of the MEMS resonator. As the voltage increases the subcritical bifurcation point A is shifted significantly to lower frequencies, while the supercritical bifurcation point B is not significantly shifted in any way. One can notice that the range of frequencies (between points A and B) for which the resonator settles to nonzero amplitudes from any initial amplitude, increases. Also as the voltage increases the range of frequencies (between points C and B) for which the resonator can potentially (depending on the initial amplitude) reach pull-in or nonzero amplitudes decreases. Increasing the voltage has an inverse effect on the pull-in instability point D than increasing the damping. As the voltage increases point D is shifted to higher frequencies reducing the range of frequencies (between points B and D) of nonzero amplitudes.

Fig. 6 illustrates the effect of the fringe coefficient,  $f$ , on the frequency response. Fringing fields emanating from the lateral and top surfaces of the deformable beam need to be accounted for when modeling the electrostatic field. For wide beams with beam width to air gap ratio greater than 1.5, the fringing fields are usually neglected [27]. Increasing the fringe coefficient

(decreasing the width of the cantilever for the same gap distance) from a value of 0.26 to 0.5 shifts to lower frequencies the subcritical bifurcation point *A*, and point *C*. It also shifts to larger frequencies the pull-in instability point *D*, and does not have a significant influence on the supercritical bifurcation point *B*. The increase in fringe coefficient has the same effect as increasing the voltage parameter, except the range of frequencies (between points *C* and *B*) for which the resonator potentially reaches (depending on the initial amplitude) pull-in or nonzero amplitudes. This range increases with the increase of the fringe coefficient while it was decreasing with voltage increase. One can notice that if the fringe effect is neglected  $f=0$  then the supercritical bifurcation point *B* is not affected, but the frequencies of all others points *A*, *C*, and *D* are not correctly predicted. Ignoring the fringe effect results in higher frequency of the subcritical bifurcation point *A*, lower frequency of point *D*, and higher frequency of point *C*. This leads to erroneous ranges of frequencies for (1) nonzero amplitudes (between frequencies of points *B* and *D*), (2) pull-in and nonzero amplitudes (between points *B* and *C*), and (3) nonzero amplitudes from any initial amplitude (between points *A* and *B*).

In conclusion when comparing MMS and ROM, although accurate for small amplitudes, MMS fails to accurately predict the behavior of the resonator for large amplitudes. If five terms are used, the ROM method is able to accurately predict the behavior of the MEMS resonator for all amplitudes. Also, the use of the AUTO 07P provides accurately the pull-in instability point *D* and the lower frequency of the unstable branch, point *C*, of the subcritical bifurcation.

The results of this paper are valid for (1) MEMS cantilevers of width to thickness ratio greater than five, and gap to thickness ratio greater than two [18,19,27] since Palmer formula for electrostatic force is used, and (2) Euler–Bernoulli cantilevers (thickness to length ratio greater than hundred). Future directions of research include the effects of imperfections, and noise on the response of the structure.

Practical implications of this paper are: (1) more sensing information can be acquired by using the two bifurcation points *A* and *B* and the pull-in instability point *D* in Fig. 2 by sweeping up and down the frequency, (2) there is a significant range of frequencies, between points *B* and *C*, for which, if enough large initial amplitude (above branch *AC*), the system reaches high amplitudes or pull-in, and (3) if zero initial amplitude and fixed frequency, then pull-in phenomenon does not occur, Fig. 2.

## Acknowledgements

This material is based on research sponsored by Air Force Research Laboratory under Agreement number FA8650-07-2-5061. The U.S. Government is authorized to reproduce and distribute reprints for Governmental purposes notwithstanding any copyright notation thereon. The views and conclusions contained herein are those of the authors and should not be interpreted as necessarily representing the official policies or endorsements, either expressed or implied, of Air Force Research Laboratory or the U.S. Government.

## References

- [1] M.I. Younis, E.M. Abdel-Rahman, A.H. Nayfeh, A reduced-order model for electrically actuated microbeam-based mems, *J. Microelectromech. Syst.* 12 (5) (2003) 672–680.
- [2] K. Vummidi, M. Khater, E.M. Abdel-Rahman, A.H. Nayfeh, S. Raman, Dynamic pull-in of shunt capacitive MEMS switches, *Procedia Chem.* 1 (2009) 622–625.
- [3] M. Gurbuz, T.F. Parlak, A. Bozhurt Bechteler, An analytical design methodology for microelectromechanical (MEM) filters, *Sens. Actuators A* 119 (2005) 38–47.
- [4] W. Zhang, R. Baskaran, K.L. Turner, Effect of cubic nonlinearity on auto-parametrically amplified resonant MEMS mass sensor, *Sens. Actuators A* 102 (2002) 139–150.
- [5] W. Zhou, A. Khaliq, Y. Tang, H. Ji, R.R. Selmic, Simulation and design of piezoelectric microcantilever chemical sensors, *Sens. Actuators A* 125 (2005) 69–75.
- [6] F.M. Al Saleem, M.I. Younis, L. Ruzziconi, An experimental and theoretical investigation of dynamic pull-in in MEMS resonators actuated electrostatically, *J. Microelectromech. Syst.* 19 (4) (2010) 794–806.
- [7] S. Krylov, I. Harari, Y. Cohen, Stabilization of electrostatically actuated microstructures using parametric excitation, *J. Micromech. Microeng.* 15 (2005) 1188–1204.
- [8] F. Al Saleem, M. Younis, Controlling dynamic pull-in escape in electrostatic MEMS, in: *Proceeding of the 6th International Symposium on Mechatronics and its Applications (ISMA 09)*, Sharjah, UAE, March 24–26, 2009.
- [9] J. Stulemeijer, J.A. Bielen, P.G. Steeneken, J. Bouwe van der Berg, Numerical path following as an analysis method for electrostatic MEMS, *J. Microelectromech. Syst.* 18 (2) (2009) 488–499.
- [10] A.H. Nayfeh, M.I. Younis, E.M. Abdel-Rahman, Dynamic pull-in phenomenon in MEMS resonators, *Nonlinear Dyn.* 48 (2007) 153–163.
- [11] J. Nee, Nonlinear problems arising in electrostatic actuation in MEMS, *J. Math. Anal. Appl.* 352 (2009) 836–845.
- [12] M. Mojahedi, M.M. Zand, M.T. Ahmadian, Static pull-in analysis of electrostatically actuated microbeams using homotopy perturbation method, *Appl. Math. Model.* 34 (2010) 1032–1041.
- [13] M.M. Zand, M.T. Ahmadian, B. Rashidian, Semi-analytic solutions to nonlinear vibrations of microbeams under suddenly applied voltages, *J. Sound Vib.* 325 (2009) 382–396.
- [14] H.M. Ouakad, M.I. Younis, The dynamic behavior of MEMS arch resonators actuated electrically, *Int. J. Non-Linear Mech.* 45 (2010) 704–713.
- [15] M.I. Younis, E.M. Abdel-Rahman, A.H. Nayfeh, Global dynamics of MEMS resonators under superharmonic excitation, in: *Proceedings of the 2004 International Conference on MEMS, NANO and Smart Systems (ICMENS'04)*, IEEE, 2004.
- [16] A.H. Nayfeh, H.N. Arafat, Nonlinear response of cantilever beams to combination and subcombination resonances, *J. Shock Vib.* 5 (1998) 277–288.
- [17] E.M. Abdel-Rahman, A.H. Nayfeh, M.I. Younis, Dynamics of an electrically actuated resonant microsensors, in: *Proceedings of the International Conference on MEMS, NANO and Smart Systems (ICMENS'03)*, IEEE, 2003.
- [18] D.I. Caruntu, I. Martinez, K.N. Taylor, Voltage-amplitude response of alternating current near half natural frequency electrostatically actuated MEMS resonators, *Mech. Res. Commun.* 52 (2013) 25–31.
- [19] D.I. Caruntu, I. Martinez, M.W. Knecht, ROM analysis of frequency response of AC near half natural frequency electrostatically actuated MEMS cantilevers, *J. Computational Nonlinear Dyn.* 8 (2013) 031011-1–031011-6.
- [20] D.I. Caruntu, M.W. Knecht, On nonlinear response near half natural frequency of electrostatically actuated microresonators, *Int. J. Struct. Stab. Dyn.* 11 (4) (2011) 641–672.
- [21] D.I. Caruntu, Eigenvalue singular problem of factorized fourth-order self-adjoint differential equations, *J. Appl. Math. Computation* 224 (2013) 603–610.
- [22] D.I. Caruntu, Factorization of self-adjoint ordinary differential equations, *J. Appl. Math. Computation* 219 (2013) 7622–7631.
- [23] D.I. Caruntu, Dynamic modal characteristics of transverse vibrations of cantilevers of parabolic thickness, *Mech. Res. Commun.* 33 (3) (2009) 391–404.
- [24] D.I. Caruntu, Classical Jacobi polynomials, closed-form solutions for transverse vibrations, *J. Sound Vib.* 306 (3–5) (2007) 467–494.
- [25] D.I. Caruntu, M.W. Knecht, On nonlinear response of capacitive sensors, in: *Proceedings of the ASME Design Engineering Technical Conference*, vol. 6, 2009, pp. 531–538.
- [26] E.J. Doedel, B.E. Oldeman, AUTO-07P: Continuation and Bifurcation Software for Ordinary Differential Equations, Concordia University, Montréal, Canada, 2009.
- [27] R. Batra, M. Porfiri, D. Spinello, Electromechanical model of electrically actuated narrow microbeams, *J. Microelectromech. Syst.* 15 (5) (2006) 1175–1189.